

Parametric Self-Oscillation via Resonantly Enhanced Multiwave Mixing

A. S. Zibrov^{1,4,*}, M. D. Lukin², and M. O. Scully^{1,3}

¹*Dept. of Physics, Texas A & M University, College Station, TX 77843*, ²*ITAMP, Harvard-Smithsonian Center for Astrophysics, Cambridge, MA, 02138*, ³*Max-Planck Institut für Quantenoptik, D-85748 Garching, Germany*, ⁴*Lebedev Institute of Physics, Moscow, Russia*

Abstract

We demonstrate an efficient nonlinear process in which Stokes and anti-Stokes components are generated spontaneously in a Raman-like, near resonant media driven by low power counter-propagating fields. Oscillation of this kind does not require optical cavity and can be viewed as a spontaneous formation of atomic coherence grating.

PACS numbers: 42.50.-p;42.65.-k;42.50.Gy

Typeset using REVTeX

*present address: National Institute of Standards and Technology, Boulder, Colorado, 80303

Theoretical and experimental work of past few years on atomic coherence and interference has demonstrated a potential to improve significantly the existing nonlinear optical techniques [1]. In the present Letter we demonstrate efficient parametric generation accompanying the *spontaneous* formation of the coherent superposition states. Specifically, the present work reports the observation of the spontaneous parametric self-oscillation in resonant Raman media. Such generation does not involve optical cavity and appears under remarkably simple circumstances, when two low-power counter-propagating fields interact with the medium. Oscillation manifests itself as Stokes and anti-Stokes components generated with a frequency shift corresponding to that of the Raman transition. As the oscillator goes over threshold, dramatic increase and narrowing of the beat note between the input field and generated components takes place.

The principal possibility of mirrorless parametric oscillation with counter-propagating signal and idler fields has been suggested in 1960's by Harris [2]. The original proposal based on non-degenerate frequency mixing has not been realized up to now due to small values of nonlinearities in available materials and difficulties in achieving phase matching [3]. It is easier to achieve mirrorless oscillation in degenerate four-wave mixing. The possibility of self-oscillation in such interactions has been predicted in [4], and a number of the related effects, such as conical emission or transverse pattern formation have been observed in a vapor driven by very strong, off-resonant counter-propagating laser beams [5]. Workers in the field have also noted the importance of Raman nonlinearities in the early experiments on polarizations instabilities [6].

As compared to the above work the presently reported results utilize atomic coherence gratings [7,8] in a resonant double- Λ atomic system (Fig.1a). Coupling of counter-propagating Stokes and anti-Stokes fields via such a grating appears to be the main physical mechanism resulting in Raman self-oscillation [8]. Similar to several related studies [1,7,9,10] the present work operates in a so-called strong coupling regime in which nonlinearities can not be derived from a usual perturbation expansion. In this regime quantum coherence and interference have a profound influence on nonlinear parametric amplification. For ex-

ample, linear and non-linear absorption of parametrically generated fields can be controlled and the phase mismatch, inherent in all non-degenerate parametric interactions involving counter-propagating fields, can be easily compensated by a large dispersion accompanying resonances in phase-coherent media. It is important that due to quantum interference the strong-coupling regime was reached in the present work with a very low driving power. The present results are therefore directly related to recent theoretical studies on few photon quantum control [11], switching [12], and quantum noise correlation [13], and can potentially be used to study interactions of a very low-energy fields and for suppression of quantum noise. Moreover, if extended to resonant molecular vapor the present approach might be useful for efficient Raman frequency shifting. Likewise, narrow-linewidth signals may also be of interest e.g. for optical magnetometry.

The present experiments follows our previous work on atomic coherence effects in optically driven Λ systems in Rb [10,14]. Studying the detailed lineshape of these signals, we found that under certain conditions the Raman amplification [14] can actually turn into a coherent self-oscillation of the Stokes and anti-Stokes components. An essential element for the oscillation to appear is the existence of the two driving fields (E_f, E_b) propagating in the opposite directions. We first discovered this oscillation as the result of simple Fresnel reflection from the rear window of the Rb cell. Figure 1b shows the simplest experimental configuration that produced Raman oscillation. A beam from an extended-cavity diode laser passes successively through an optical isolator (I), a focusing lens, a heated Rb cell, a partially reflecting mirror and onto a fast photodiode (PD). The signal from the photodiode is detected using a microwave spectrum analyzer (SA). The partially reflecting mirror (M) is used to retro-reflect some of the transmitted beam back through the Rb vapor. With proper tuning of laser frequency, the backward beam causes the Raman gain peak to grow to the point of oscillation threshold. When the self-oscillation occurs the detected Raman beatnote signal at a frequency of hyperfine splitting (ω_{hfs}) increases in amplitude by as much as 60dB and its linewidth narrows from 200 kHz to less than 300 Hz (Fig.2a). Under appropriate conditions the beatnote linewidths as narrow as 100 Hz FWHM were observed

(Fig.3a). This is much narrower than the usual broadening mechanisms for Raman transitions under the present conditions (primarily, transit broadening $\gamma_{bc} \sim 50$ kHz and power broadening ~ 500 kHz). The oscillation occurs without any cavity enclosing the cell. We have been careful to eliminate possible extraneous sources of feedback to lasers or other optical and electronic elements.

In order to study the physical origin of the oscillation process we carried out a series of experiments, where instead of reflecting the incident laser light we injected laser beams with different frequencies from the opposite directions (Fig.1c). We found that the oscillation occurs readily if the forward and backward fields are tuned to the different ground state hyperfine level as diagramed in Fig.1a. It is more difficult to make the system oscillate if the backward beam is tuned to the same frequency as the forward beam. If tuned to different ground state hyperfine levels, the oscillation was observed with the backward beam coupling either the same ($P_{1/2}$) or different ($P_{3/2}$) upper-state fine-structure levels as the forward beam. In our two-laser experiments it was easy to see oscillation for both ^{85}Rb and ^{87}Rb isotopes. When oscillating, the Rb vapor can convert as much as 4% of the total input power into the frequency shifted Stokes and anti-Stokes sidebands.

Typical conditions to observe the oscillation with a single laser beam are: ECDL tuned in the wing of the Doppler profile of the ^{85}Rb , D1 line (F=2 to F'=3) transition, ~ 10 mW of power in spot size about ~ 500 microns, 5 cm long Rb cell operated at 75-95 C, and between 10 and 80 % of the driving power is retro-reflected back through the Rb cell. In the two-laser experiments oscillation was observed for driving input powers 2 – 10 mW, spot sizes 0.1 – 2mm, and cell temperatures 65 – 100°C.

The oscillation frequency shift (ω_0) does change somewhat with laser tuning (typical case was 30 Hz per MHz of laser tuning) and with angle between the forward and backward beams [15]. However, the oscillation frequency always remains within the bandwidth (few hundred kHz) of the power broadened and shifted single-beam Raman gain peak. The oscillation prefers, but does not necessarily require a circularly polarized beam, and the gain is largest with zero applied magnetic field.

We have analyzed the characteristics of the forward and backward beams by making beatnotes with independently tuned laser sources, and by using optical cavities to analyze the spectra. We found that the field components at frequencies of the forward and backward driving fields (ν_f or ν_b) are surrounded by generated first order Stokes and anti-Stokes fields at frequencies $\nu_{f,b} \pm \omega_0$. In certain cases second order components have been seen as well. The generated components produce, in general, asymmetric spectrum. In particular, in cases when forward driving field is tuned to e.g. upper ground state hyperfine sublevel and backward driving beam is tuned to the lower hyperfine sublevel, the anti-Stokes component observed in a forward direction is much more ($\sim 20 - 30\text{dB}$) intense than the Stokes one.

These observations suggest that the actual oscillation mechanism is somewhat different from (although related to) that studied theoretically in Ref. [8]. That work involved only one pair of counter-propagating components. Motivated by experimental results, we consider a theoretical model in which atoms in a double Λ -type configuration are interacting with six optical fields. These include two counter-propagating driving fields with frequencies ν_F, ν_B and complex slowly varying amplitudes \mathcal{E}_F and \mathcal{E}_B ; anti-Stokes and Stokes components with frequencies $\nu_{1,3} = \nu_F \pm \omega_0$ propagating in the forward direction ($\mathcal{E}_1, \mathcal{E}_3$), and corresponding components with frequencies $\nu_{2,4} = \nu_B \pm \omega_0$ propagating in the backward direction ($\mathcal{E}_2, \mathcal{E}_4$). The field is then written as $E = \sum_i (\mathcal{E}_i e^{-i(\nu_i t + k_i r)} + \text{c.c.})/2$. Below we focus on the linear theory describing the oscillation threshold. Hence, all generated components are treated to first order only and saturation effects are disregarded. These assumptions allow us to truncate the infinite hierarchy of equations. The resulting polarization can be written in the form $P = \sum_i (\mathcal{P}_i e^{-i(\nu_i t + k_i r)} + \text{c.c.})/2$. We are interested here in polarizations at the Stokes and anti-Stokes frequencies, which are related to the field components by 4×4 susceptibility matrix χ_{mn} : $\bar{\mathcal{P}}_m = \epsilon_0 \chi_{mn} \exp(ik_{mn}r) \bar{\mathcal{E}}_n$, where $\bar{\mathcal{P}} = [\mathcal{P}_1, \mathcal{P}_2, (\mathcal{P}_3)^*, (\mathcal{P}_4)^*]^T$, $\bar{\mathcal{E}} = [\mathcal{E}_1, \mathcal{E}_2, (\mathcal{E}_3)^*, (\mathcal{E}_4)^*]^T$, and k_{ij} are representing free-space wave vector mismatch. For the present problem the matrix elements of $[\chi]$ were calculated explicitly for each velocity group and averaged over Maxwellian velocity distribution. In the present calculations we consider fields interacting in a slab of medium of the length L . Assuming that the solution

is homogeneous in transverse directions leads to $(k_{ij})_{\perp} = 0$, and the evolution along the longitudinal direction z is described by: $\frac{\partial}{\partial z}\mathcal{E}_i = i/(2\epsilon_0)(k_i)_z\mathcal{P}_i$. The appropriate boundary conditions are taken to include a weak “seed” input (\mathcal{E}) at anti-Stokes frequencies (corresponding to e.g. spontaneous emission, or vacuum field).

Before proceeding with comparison of experiment and theory we illustrate the origin of the oscillation. To this end, let us assume that absorption of the driving fields is negligible, and there is no inhomogeneous broadening. Furthermore, we disregard the coupling of the forward (backward) driving field with all transitions except for $c \rightarrow a$ ($b \rightarrow a'$) and assume that the detuning of the backward driving field from respective single photon resonance (Δ_B) is much larger than the corresponding detuning of the forward drive. In such a situation only forward anti-Stokes (\mathcal{E}_1) and backward Stokes (\mathcal{E}_4) fields are involved into nonlinear interaction (Fig.4a, [8]). In this case: $\partial\bar{\mathcal{E}}_i/\partial z = a_{ij}\bar{\mathcal{E}}_j$, with $\{i, j\} = \{1, 4\}$ and $a_{11} = -\eta_1[\gamma_{bc} + i(\omega_0 - \omega_{hfs}) + i(|\Omega_B|^2 - |\Omega_F|^2)/\Delta_B]/|\Omega_F|^2 - ik_{11}$, $a_{14} = i\eta_1[\Omega_B\Omega_F/(\Delta_B|\Omega_F|^2)]$, $a_{41} = i\eta_4[\Omega_B^*\Omega_F^*/(\Delta_B|\Omega_F|^2)]$, $a_{44} = -ik_{41}$. Here $\eta_i = (k_i)_z 3/(8\pi^2)N(\lambda_i)^3\gamma_i$, where λ_i is a wavelength of the i th field component and γ_i is the radiative decay rate on the transition coupled by this component of the field. N is atomic density, and $\Omega_{F,B}$ are Rabi-frequencies.

When the phase matching condition is satisfied ($\text{Im}(\delta a) = 0$, $\delta a \equiv (a_{11} - a_{44})/2$), we find:

$$\mathcal{E}_1(L) \sim \mathcal{E}_4(0)^* \sim \frac{\mathcal{E}}{\delta a \sin(sL) - s \cos(sL)}, \quad (1)$$

where $s = \sqrt{a_{14}a_{41} - (\delta a)^2}$, and the unimportant proportionality constants have absolute values of the order of unity. These solutions diverge if $\tan(sL) = s/(\delta a)$, which indicates the onset of mirrorless oscillations. Note that the latter condition can be satisfied if $\eta_4|\Omega_F\Omega_B| > \eta_1\gamma_{bc}|\Delta_B|$, which is identical to a strong coupling condition of Refs. [1,7–14]. Let us examine now the phase matching. Close to the two-photon resonance we have:

$$\kappa(\omega_0 - \omega_{hfs} - \xi) + c[k_f + k_b - k_1 - k_4]_z = 0, \quad (2)$$

where $\xi = (|\Omega_F|^2 - |\Omega_B|^2)/\Delta_B$ is a function of drive power and detunings representing a light shift, and $\kappa = c\eta_1(k_1)_z/|\Omega_F|^2$. It is interesting that this equation resembles closely the

frequency pulling equation of the usual laser theory, with frequency stabilization coefficient κ . The first term in the left-hand side corresponds to atomic dispersion, and the second describes the geometrical phase mismatch. This contribution is proportional to the Raman transition frequency (see inset to Fig.4) and also depends on relative angles between driving beams. Hence it plays a role analogous to the cavity shift. Note, however, that under the typical oscillation conditions stabilization coefficient $\kappa \sim c/(\gamma_{bc}L) \gg 1$ and the oscillation frequency is locked to the light-shifted Raman transitions frequency.

This implies that in the example considered above the physics behind the oscillation phenomenon is the coupling of the counter-propagating Stokes and anti-Stokes fields via spontaneously created atomic coherence ρ_{bc} . On one hand such coupling results in scattering of these fields into each other, thus forming an effective feedback. On the other hand, this process is also accompanied by parametric amplification. When both of the effects are present self-sustained oscillation can occur.

Let us consider the influence of other nonlinear processes on mirrorless oscillation. When only a forward driving field is present nonlinear interaction results in the coupling between forward (or backward) propagating Stokes and anti-Stokes fields (Fig.4b) leading to coherent Raman scattering and amplification of the co-propagating pair of fields in the vicinity of two-photon resonance [8,9]. Oscillation is not possible in this case, since no effective feedback is present. However, when coherent Raman scattering exists in addition to the coupling between counter-propagating Stokes and anti-Stokes components, it can result in lowering the oscillation threshold. The process shown in Fig.4c represents a different type of parametric interaction. It leads to the scattering of the counter-propagating anti-Stokes (or Stokes) waves into each other, which does not change the total photon number of weak fields. Consequently, it alone can never lead to the oscillations. However, oscillations can emerge if in addition to the parametric energy exchange additional amplification mechanisms (e.g. coherent Raman scattering) are present.

In general, for the detailed comparison of the theory and experiment all of the six processes of the type shown in Fig.4 should be taken into account. They give rise to simultaneous

generation of all components in both directions. To make a comparison we have solved the full system of propagation equations numerically, taking into account Doppler broadening, and propagation of all fields. The results (Fig.2b) show good qualitative agreement with experiments.

This work would not have been possible without active involvement and contributions of L. Hollberg and V. Velichansky. The authors warmly thank them as well as M. Fleischhauer, P. Hemmer, S. Harris, A. Matsko, V. Sautenkov, and G. Welch for useful discussions, and T. Zibrova for valuable assistance. We gratefully acknowledge the support from the Office of Naval Research, the National Science Foundation, and the Air Force Office of Scientific Research.

REFERENCES

- [1] S. E. Harris, J. E. Field, and A. Imamoglu, Phys. Rev. Lett. **64**, 1107 (1990); M. Jain *et al.*, Phys. Rev. Lett. **77**, 4326 (1996); for review see S. E. Harris, Physics Today **50**, # 7, 36 (1997).
- [2] S. E. Harris, Appl. Phys. Lett., **9**, 114 (1968)
- [3] Y. R. Shen, *The Principles of Nonlinear Optics* (John Wiley & Sons, 1984).
- [4] A. Yariv, D. Pepper, Opt.Lett. **1**, 16 (1977).
- [5] See e.g. special issue on *Transverse Effects in Nonlinear-Optical Systems*, J. Opt. Soc. Am. B **7**, 948-1157 (1990); **7**, 1264-1373 (1990); M.Ducloy and D.Bloch, in *Optical Phase Conjugation*, p. 98, M. Gower, and D. Proch Eds., (Springer, 1994).
- [6] D. Gauthier *et al.*, Phys. Rev. Lett. **61**, 1827 (1988); *ibid* **64**, 1721 (1990).
- [7] P. R. Hemmer *et al.*, Opt. Lett. **20**, 982 (1995).
- [8] M. D. Lukin, P. Hemmer, M. Loeffler, and M. O. Scully, Phys. Rev. Lett. **81**, 2675 (1998).
- [9] K. Hakuta, M. Suzuki, M. Katsuragawa, and J. Z Li, Phys. Rev. Lett. **79**, 209 (1997).
- [10] M.D.Lukin *et al.* Phys.Rev.Lett. **79**, 2959 (1997).
- [11] A. Imamoglu, H. Schmidt, G. Woods, and M. Deutsch, Phys.Rev.Lett. **79**, 1467 (1997); M. Dunstan *at al.*, in *Proc.: Quantum Communication, Computing, and Measurement 2*. P. Kumar, G.M. D'Ariano, and O. Hirota Eds.
- [12] S. Harris and Y. Yamamoto, Phys.Rev.Lett. **81**, 3611 (1998).
- [13] M.D.Lukin *et al.* Phys.Rev.Lett. **82**, 1847 (1999).
- [14] A.S.Zibrov *et al.*, in *Proc. 5th Simposium on Frequency Standards and Metrology'*, J.C.Bergquist Ed., (World Scientific, 1996).

[15] When the gain is high it is possible to have comb of oscillations with spacings between modes that could be tuned from 10's to 100's of kHz. This subsidiary comb structure depends strongly on angle of the return beam, the laser frequency, and is correlated with spatial mode changes in the generated light.

FIGURES

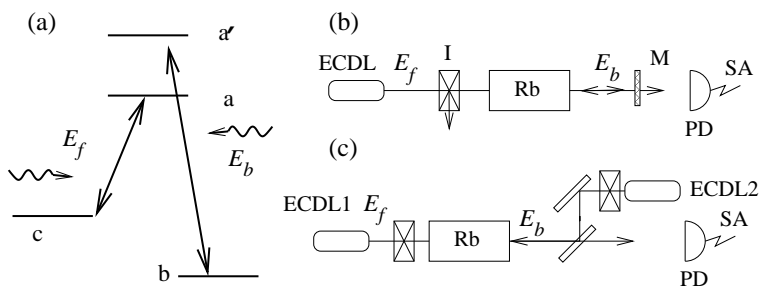


FIG. 1. (a) A prototype 4-level model for self-oscillations. In general, we assume that each driving field couples both of the ground states. The upper levels of this double- Λ system can represent some manifolds of states. In a particular case, a and a' can also represent an identical state. In the experiment states c and b are hyperfine sublevels of the Rb ground state $5S_{1/2}$. (b,c) Experimental setups (schematic).

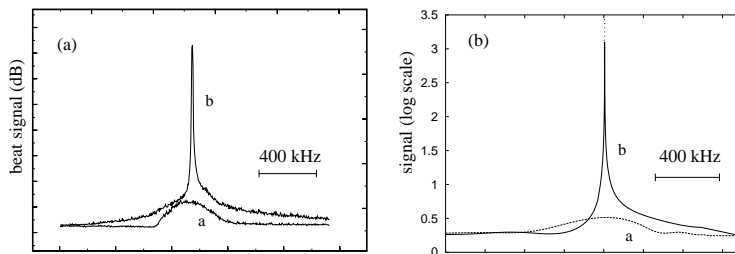


FIG. 2. a) A typical signal recorded by a fast photo-diode. Curve a is recorded with only forward driving beam present. Self-oscillations occur in the presence of the forward and backward driving fields (curve b). Parameters are: cell temperature 92°C ; forward driving beam with power 10 mW and spot size 1.5 mm is detuned by 800 MHz to the red side of $F = 3 \rightarrow F' = 3'$ transition of D_1 line; backward driving beam with power 2.5 mW and spot size 1.5 mm is detuned by 2 GHz to the blue side of $F = 2 \rightarrow F'' = 3''$ transition of D_2 line. b) Calculated signals corresponding to the experimental conditions of Fig.2a. (At the point corresponding to parametric oscillation linear theory predicts infinite growth).

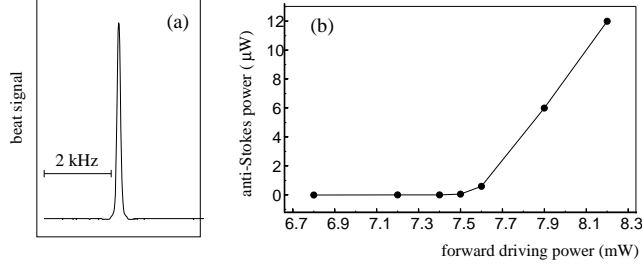


FIG. 3. a) A typical beat signal at 3.034 GHz recorded when the frequency of the driving laser is locked to a reference cavity. b) A typical dependence of the generated anti-Stokes power as a function of the input driving power in a vicinity of oscillation threshold.

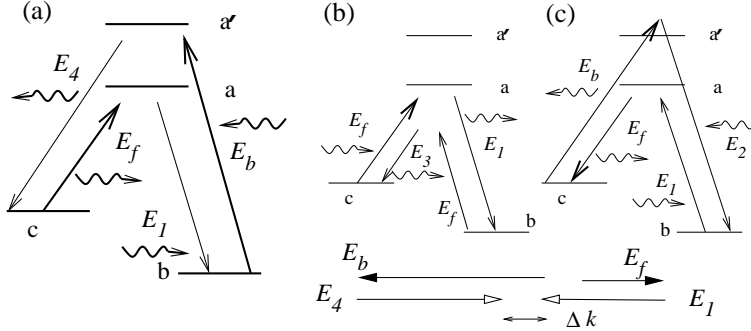


FIG. 4. Examples of different types of nonlinear processes contributing to self-oscillations. a) Direct nonlinear coupling between counter-propagating Stokes and anti-Stokes fields; b) Coherent Raman scattering; c) Parametric energy exchange between counter-propagating anti-Stokes fields. For each of the processes (a-c) there exists a complimentary process of the same type involving other pair of weak fields (e.g. $E_{2,3}$ in Fig.4a). Inset illustrates wave vector mismatch for the process (a). If all fields are propagating along the z axes $[k_0^F + k_0^B - k_1 - k_4]_z = 2\omega_0/c$.